Modeling of Impact Damage of Sewing Machine Needle on Woven Fabric by Finite Element Method

Nader Khadamalhosseini, Mohammad Nasr-Isfahani, Masoud Latifi and Saeed Shaikhzadeh-Najar

Abstract—**The purpose of the present work is to develop a computational model to simulate the effect of sewing machine needle impact on woven fabrics. This research presents a finite element model of woven fabric using commercial finite element software (ABAQUS 6.8). In the model, the orthotropic properties of the fabric, the elastic nature of the yarn, the sliding contact between yarns and yarn breakage are included while employing solid elements. Experimental works are also performed to compare with the simulation results. In order to quantify the damage of woven fabrics punched by sewing needles in experimental and simulation work, a damage index is introduced. Same trends in experimental and simulation results reveal that the model can quantitatively differentiate the damage of fabrics impacted by sewing machine needles.**

Key words: Simulation, finite element, sewing machine, needle, woven fabric.

I. INTRODUCTION

MACHINE sewing process is used to produce a wide range of textile products. Sewing quality for some technical textiles like automobile airbag, parachute and protective cloths plays an important role in the safety and health of people. Thus, it seems to be necessary to demonstrate an accurate method for measuring and analysis of fabric damages that occur during machine sewing process.

For studying sewing process Gotlih [1], Stylios [2] and Lomov [3] measured the sewing forces using analytical methods with lots of simplification in solution and boundary conditions. Mallet and Du [4] used FEM to analyze sewing needle forces and measured the deformation of fabric specimens.

Textile fabrics were modeled in different ways to analyze their impact behavior which is similar to swing process. Roylance, [5] modeled fabric, using finite-difference method, as an assembly of pin-jointed, mass less fiber elements. Tan [6] and Legrand [7] idealized fabric as a network of one-dimensional elements that were interconnected at crossover points. In another work, Tan [8] simulated the fabric as a network of visco-elastic beam elements and a three-element visco-elastic model in which yarns can slip at crossover points. Lim [9] (2003) and Shim [10] (2001) investigated the finite-element simulation of ballistic impact on fabric based on a continuum shell, which incorporates visco-elasticity and rate-sensitive failure criterion.

In this study, the impact of sewing machine needle on a real woven fabric is simulated by commercial finite element package (ABAQUS 6.8), and compared with experimental results. Three models with different needle sizes are developed in order to compare their results with those obtained from the experimental method. In the presented model, the orthotropic properties of the fabric, the elastic nature of the yarn, the sliding contact between yarns and yarn failure are included and solid elements under low-speed impact are utilized.

II. EXPERIMENTAL METHOD

Many parameters like mechanical and geometrical properties of sewing needle surface and fabric are required to be simulated in sewing process.

A. Material and Equipments

In this study, in order to illustrate the effect of needle impact on, viscose woven fabric was used. Warp and weft yarns were two ply white viscose yarns. Table I shows the structural properties of the used fabric.

TABLE I
STRUCTURAL PROPERTIES OF FABRIC

Woven Fabric	Fabric density (ENDS/CM)	Mass of unit area (gr/m^2)	Fabric thickness (mm)	Weave type
Warp ends	43	196.5	0.38	plain
Weft ends	26			

B. Damage Evaluation Method

In this study, with inspiration of the sewability test method applied by Fredric [11], a new approach was innovated for the evaluation of fabric yarn's damage due to sewing needle impact operation. All fabric samples were carefully cut between two consecutive stitch holes. Six weft and warp yarns from the impact area were pulled out of the fabric for 10 consecutive holes. In continuation, the appearance of pulled-out yarns was visually inspected and divided to three groups related to their damaging degrees. First group was fractured yarns which were rent apart during pulling out of fabrics. Partial fractured yarns, which were rent apart with a little tension, were categorized as the second group. Third group consisted of yarns deformed while the needle was piercing on the fabric and their strengths were not considerably decreased. In order to quantify a damage index, each pulled-out yarn in the first, second and third group is weighted 1, 0.5 and 0.1 respectively. Finally, the damage index for each stitch hole

N. Khadamalhosseini, M. Nasr-Isfahani, M. Latifi, and S. Shaikhzadeh-Najarare are with the Department of Textile Engineering, Textile Research and Excellence Centers, Amirkabir University of Technology, Tehran, Iran. Correspondence should be addressed to M. Latifi (e-mail: latifi@aut.ac.ir).

was calculated applying Eq. (1).

$$DIESH = ((NFY * 1) + (NPFY * 0.5) + (NDY * 0.1))/6 \quad (1)$$

where, DIESH shows damage index for each stitch hole, NFY indicates the number of fractured yarn, NPFY and NDY are the number of partial fractured yarn and the number of deformed yarn, respectively.

Table II shows the result of the experimental method for 6 specimens.

TABLE II
EXPERIMENTAL RESULTS OF DAMAGE EVALUATION FOR 10 STITCH HOLES EACH OF WHICH INCLUDES 6 YARNS (APPLYING EQUATION 1 FOR EACH HOLE) EXPERIMENTAL TESTS

Sample #	Needle code	Sewing direction	AFY*	APFY♦	ADY∇	DI● (fy+pfy+dy)/6
1	90/14	Weft	0.100	0.083	0.03	0.213
2	100/16	Weft	0.100	0.100	0.033	0.233
3	110/18	Weft	0.033	0.200	0.027	0.26
4	90/14	Warp	0.100	0.117	0.067	0.284
5	100/16	Warp	0.133	0.183	0.073	0.389
6	110/18	warp	0.266	0.167	0.077	0.510

*: Assessment of Fractured Yarns, ♦: Assessment of Partial Fractured Yarns,
∇: Assessment of Deformed Yarns, ●: Damage Index.

To determine the simulation parameters, the tensile test for the measurement of Yang modulus and breaking load, and yarn strength test were performed according to ASTM D2256-02 test method on Instron tensile tester. Warp and weft count were also measured according to ASTM D1059-01. The geometrical and mechanical properties of fabric yarns required for simulation process are shown in Table III.

As shown in Table III, the obtained tensile modulus and tensile load at breakage for warp yarns are lower than weft yarns. This result is supposed to be because of different tensions sustained in yarns during weaving operation.

III. FINITE ELEMENT MODEL OF SEWING

The fabric, yarn and sewing parameters were used to model the sewing operation.

A. *Geometrical Model of Warp and Weft Yarns*

Two 3D models were constructed for warp and weft yarns of the fabric applying the geometrical properties obtained in experimental tests. The deformable solid element was employed to form the models and two sweep Spline curves were used to configure the yarn waves. Figure 1 shows the simulated warp and weft yarns.

As shown in Figure 1 the warp wave domain is much longer than weft wave domain. This is because of the large deference (difference) between warp and weft density in the fabric. Homogeneous elements were applied in the yarn model for the representation of its linear and nonlinear behavior.

B. *Introduction of Mechanical Properties of Simulated Yarns*

Since both warp and weft yarns were made of viscose fibers, their default densities were considered to be 1.52g/cm^3.Figure 2 shows the tensile load-strain curve of warp and weft yarns tested in the experimental work.

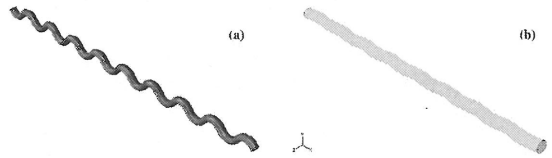

Fig. 1. 3D simulated yarns (a): warp, (b): weft.

As shown in Figure 3, both curves have a mild slope from the beginning and after one percent of strain, curves(curve's) slope is increased and finally both of the yarns are broken at about 4 percent of tensile strain with a constant slope. Mild slopes in the beginning of both curves are because of the straightening up of pulled out yarns. Thus, the modulus between two and three percent of strain was used as the initial modulus of yarns in the modeling procedure.

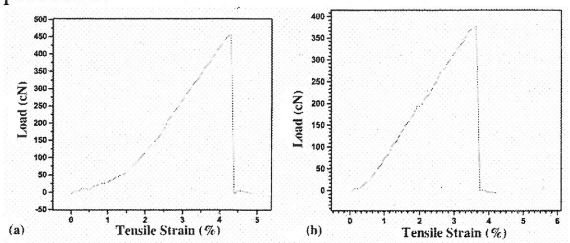

Fig. 2. Tensile load-strain curves of yarns (a) warp, (b) weft.

The yarn breaking point was also important in this study. A small plastic area was introduced after elastic zone to define the tensile behavior of yarns after the yield stress point. The area was 0.01% of elongation. If the imported load was upper than the yield point, yarns would be immediately ruptured at the end of this short area.

The Poisson coefficient of warp and weft yarns was assumed to be zero in this study [12].

C. *Model of Needle and Fabric Holding Plates*

The dimensional features of needles were measured by Projectina microscope. Three needles were modeled in CAD environment of ABAQUS as a combination of cylinders and cones considering the needles dimensions. The diameter of the cylinder was set to be the diameter of the needle rod at its thickest cross section. The sewing machine's plates, that hold the fabric from top and bottom during the motion and penetration process of the needle into the fabric, were also modeled in CAD environment of ABAQUS. Figure 3 shows 3D images of the 100/16 needle and the upper and lower fabric holders.

It was also assumed that the needles are rigid and they do not encounter any deformation during the sewing process. In order to speed up the solving process in ABAQUS, the needles were defined as "Analytical Rigid", the holders were defined as "Discrete Rigid" and all the three needles were selected to be formed by 0.01 mm thickness shells. The Analytical Rigid surface is defined by only a few geometrical nodes and is more efficient than other types.

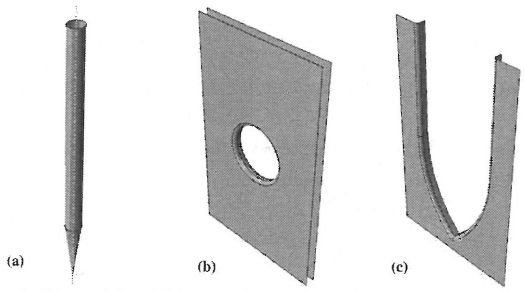

Fig. 3. 3D models of (a) 100/16 needle, (b) upper fabric holder and (c) lower fabric holder.

D. *Assembly of Modeled Parts*

The modeled parts were located in appropriate points in the assembly environment considering the geometrical properties of the simulated fabric. To initiate the process, warp and weft yarns were duplicated enough to simulate about $7_{\times}3.8$ mm^2 piece of fabric. The yarns were rotated and located in appropriate points in X-Z plane in a 3D environment. The upper and lower holder plates were then added above and below of the fabric so that they were parallel to the fabric plane with 0.19 mm distance from each other. The distance was exactly half of the fabric thickness. Finally, each modeled needle was introduced to the assembly environment so that it was parallel to the Y-axis with 2 mm distance from the original coordinates. This distance represents the location of the needle at the beginning of the motion. Figure 4 shows the 3D image of the assembled parts.

E. *Definition of Surface Interaction*

Because of the large number of assembled parts, defining the interaction characteristics for each pair of surfaces was a time consuming process and increased the solution time as well. Thus, "General Contact" option was used for all surfaces and same characteristic was defined once for all. The coefficient of friction for general contacts was assumed to be 0.19. Only at locations where the needle touched the yarns, the coefficient of friction was defined 0.38 [13].

F. *Solution Steps*

Since the needle's motion was sinusoidal, the velocity and acceleration curves were the same function of time. In this study, a second degree function for needle's motion was estimated using the interpolation method. The acceleration of the needle was achieved by taking the second derivative of its position function. Finally, it was decided to run the model in six steps. The velocity was considered to be constant the first step while during other steps the acceleration was constant.

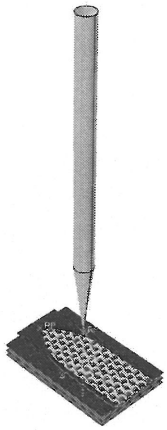

Fig. 4. 3D image of assembled parts.

G. *Boundary Conditions*

No degree of freedom was considered for the fabric holder plates. Thus the plates had no movement during the needle's motion process. In that case, the lower plate avoided the fabric moving downward during the needle's penetration into it. The upper plate does the same task in opposite direction while the needle leaves the fabric. It should be noted that at the points where the fabric and the holder plates are in contact with each other, if there is only friction resistance force, there will be a chance of fabric slipping. In real condition, this issue is resolved by exerting the spring type of force to the pressure bar. In virtual modeling environment, the problem was solved by defining the condition of tie between the crossing points of warp and weft yarns that have the shortest distance from the upper plate. The degree of freedom was set to zero for this method so that the fabric had no movement between the holding plates. On the other hand, the degree of freedom for the needle was one and it could only move along the Y-axis.

H. *Meshing Modeled Parts*

At this stage the proper element type and mesh size were separately defined for each individual part considering its function. The element type used for the yarns was hexahedral which consisted of eight nodes. The combination of rectangles and triangles which had four and three nodes was used to mesh the needle and the holding plates. Eventually, considering the type of the needle used in modeling, three models were designed and solved. The size of the needles was different in the models.

I. *Results Achieved from Modeling*

The resulted impact effect in fabric and its corresponding data for each step and node after solving the

TABLE III
GEOMETRICAL AND MECHANICAL PROPERTIES OF FABRIC YARNS

Yarn type	Yarn count (Tex)	Cross section shape	Cross section area (mm^2)	Major diameter (mm)	Minor diameter (mm)	Consecutive yarns distance (mm)	Wave length of yarn (mm)	Tensile modulus (MPs)	Tensile load at breakage (MPs)
Warp	29	Elliptical	0.0191	0.18	0.135	0.235	0.47	6751.5	225.61
Weft	28	Elliptical	0.0184	0.168	0.14	0.385	0.77	8099.3	248.30

model was stored by developing the software. Figure 5 shows the solved model of the fabric after being impacted by the 100/16 needle along the warp yarns and at the speed of 1000 RPM.

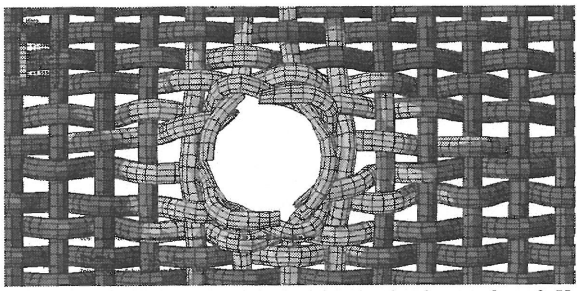

Fig. 5. Typical fabric model formed by simulated warp & weft Yarns (Figure 1) after being impacted by modeled 100/16 needle at 1000 RPM while assembled as Figure 3.

It can be observed from Figure 5 that the fabric gets damaged after hitting by the needle. The reason for this phenomenon is that the elements with defined failure criteria are damaged and their nodes are destructed when the applied stress exceeds the yielding stress of the elements. The elements which cannot tolerate the applied force and get damaged are displayed with different colors.

TABLE IV
CALCULATION OF SIMULATION INDEXES FOR FIGURE 5

Sewing Direction	AFY*	APFY♦	ADY∇	DI● (fy+pfy+dy)/6
Weft	0*1	1*0.5	1*0.1	0.100
Warp	1*1	1*0.5	4*0.1	0.317

*: Assessment of Fractured Yarns, ♦: Assessment of Partial Fractured Yarns,
∇: Assessment of Deformed Yarns, ●: Damage Index.

TABLE V
COMPARISON OF DAMAGE INDEXES RESULTED FROM SIMULATION AND EXPERIMENTAL WORKS

Needle Code	Sewing direction	EDI*	SDI●
90/14	Weft	0.213	0.033
100/16	Weft	0.233	0.100
110/18	Weft	0.26	0.117
90/14	Warp	0.284	0.183
100/16	Warp	0.389	0.317
110/18	Warp	0.51	0.353

*: Experimental Damage Index (from Table II),
●: Simulation Damage Index (applying same experimental evaluation method).

Since the numbers of fractured, damaged and deformed yarns in the numerical model are unique, in order to define comparable index, average of 6 yarns at the needle impact location were considered. The simulation damage indexes were calculated using the same equation (Eq. 1) applied for experimental works. The simulation indexes for Figure 5 are presented in Table IV.

Regarding Figure 5 and the results achieved from other two models, the empirical and simulation results are compared in Table V.

The difference between simulation and experimental indexes is due to simplifications made to simulate the model on the one hand, and inaccuracies associated with the introduced empirical method on the other hand. However, Figure 6 shows that the empirical and simulated indexes of damage for three needle types are following almost same trends (R^2=0.909).

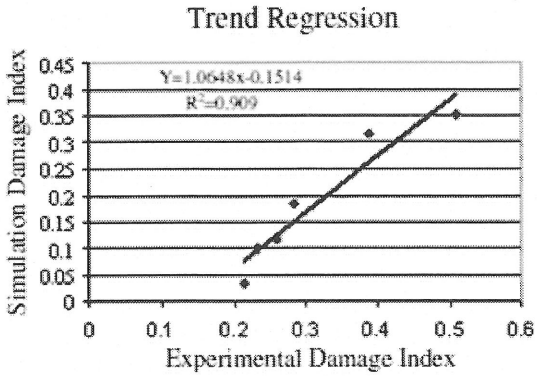

Fig. 6. Trend regression between experimental and simulation damage indexes.

IV. CONCLUSION

The results show that the damage index introduced in this work is reliable to quantify the damage of woven fabrics punched by sewing needles. Both manual and simulation procedures indicated that the needles with larger diameter increase the fabric damages.

The model developed in this study is able to simulate the impact damage of sewing machine needles on the woven fabric. The damage indexes derived from the model can be applied to compare the effect of different needle sizes on the fabric.

The introduced simulation method enables suppliers to order and/or select fabrics with proper specifications required for high quality production.

REFERENCES

[1] K. Gotlih, "Sewing needle penetration force study", *Int. J. Cloth. Sci. Tech.*, vol. 9, no. 2/3, pp. 241-248, 1997.
[2] G. Stylios and Y. M. Xu, "An investigation of the penetration force profile of the sewing machine needle point", *J. Text. I.*, vol. 86, no. 1, pp. 148-163, 1995.
[3] S. V. Lomov, "A predictive model for the penetration force of a woven fabric by a needle", *Int. J. Cloth. Sci. Tech.*, vol. 10, no. 2, pp. 91-103, 1998.
[4] E. Mallet and R. Du, "Finite element analysis of sewing process", *Int. J. Cloth. Sci. Tech.*, vol. 11, no. 1, pp. 19-36, 1999.
[5] D. Roylance, P. Hamas, J. Ting, H. Chi and B. Scott, "Numerical modeling of fabric impact", in Proc.48th ASME (AD Division), San Francisco, USA, 1995, pp. 155-160.
[6] V. B. C. Tan, V. P. W. Shim, and X. Zeng, "Modeling crimp in woven fabrics subjected to ballistic impact", *Int. J. Impact Eng.*, vol. 32, no. 1-4, pp. 561-574, 2005.
[7] X. Legrand, P. Bruniaux, and J. M. Castelain, "Fabric Modeling: Convergence Calculus Optimization", in Proc. 14th European Simulation Symposium, Dresden, pp. 459-463, 2002.
[8] V. B. C. Tan and T. W. Ching, "Computational simulation of fabric armour subjected to ballistic impacts", *Int. J. Cloth. Sci. Tech.*, vol. 32, no. 11, pp. 1737-1751, 2006.

[9] C. T. Lim, V. P. W. Shim and, Y. H. Ng, "Finite-element modeling of the ballistic impact of fabric armor", *Int. J. Impact Eng.*, vol. 28, no. 1, pp. 13-31, 2003.

[10] V. P. W. Shim, C. T. Lim and K. J. Foo, "Dynamic mechanical properties of fabric armour", *Int. J. Impact Eng.*, vol. 25, no. 1, pp. 1-15, 2001.

[11] E. B. Fredrick, "Development of a sewability test for cotton fabrics", *Text. Res. J.*, vol. 22, no.10, pp. 1952.

[12] M. Nasr-Isfahani, M. Amani-Tehran and M. Latifi, "Simulation of ballistic impact on fabric armour using finite element method", *J. Text. I.*, vol. 100, no. 4, pp. 314-318, 2009.

[13] W. E. Morton, *Physical Properties of Textile Fibers*, Manchester: Textile Institute, 1962.